benzoate resulted in formation of benzyl alcohol (5%), benzaldehyde (5%), and benzoin (1%) in addition to unreacted ethyl benzoate (85%).

Photochemical Reductions. General procedure: A benzoate ester (20 mM) and DABCO (0.1 M) were dissolved in 60 mL of ethanol and the solution was deaerated by nitrogen purge for 15–25 min. The solution was irradiated with a 450-W medium-pressure mercury lamp in a water-cooled quartz immersion well for 10 min. A sample (~2 mL) of the crude solution was taken for immediate analysis by GC and GC/MS. No reactions was observed for any of the benzoate esters in the absence of added amine. Aryl alkanes, radical coupling products, and benzoic acid were identified by comparison with authentic samples. Evaporation of solvent under reduced pressure followed by trituration of the residue with benzene afforded insoluble amonium salts.

Irradiation of benzyl benzoate for 20 min followed by workup as described indicated consumption of ~35% benzyl benzoate. The major product was obtained as a fluffy white solid, which was insoluble in benzene, identified from its spectroscopic properties as an ammonium salt of benzoic acid, $N(CH_2CH_2)_3N^+CH_2Ph\ PhCO_2^-$: NMR ($CDCl_3$) δ 8.11 (dd, 2 H, J = 3, 6.5 Hz), 7.28–7.46 (m, 8 H), 4.86 (s, 2 H), 3.57 (br t, 6 H, J = 7 Hz), 3.01 (br t, 6 H, J = 7.2 Hz). This material was photochemically and thermally unstable, and it reacted in the injector port (250 °C) of a GC apparatus to afford a neutral adduct identified by GC/MS as $PhCH_2N(CH_2CH_2)_2NCH_2CH_2OCOPh$: MS (EI) m/z (RIC) 324 (2, M^+), 202 (80, $M^+ - PhCOOH$), 189 (55), 146 (30), 105 (50, $PhCO^+$), and 91 (100, $PhCH_2^+$). Because this salt was found to decompose photochemically under the reaction conditions, the product yields were determined after ~50% conversion of benzyl benzoate. The salt formed in 70% yield, together with toluene (3%), $PhCH_2CH(OH)CH_3$ (1%), benzoic acid (~10%), and bibenzyl (16%), as quantified by GC.

Reaction of *p*-methoxybenzyl benzoate, 1-phenylethyl benzoate, benzhydryl benzoate, and *tert*-butyl benzoate afforded analogous products. Isopropyl benzoate, ethyl benzoate, and methyl benzoate did not react under these conditions, and starting materials were obtained in 90–100% recovery. The product distributions depend upon the amine used as reductant and upon the reaction conditions, and the complete results will be reported elsewhere.[68]

Acknowledgment. Support from the CSU College of Graduate Studies Research and Creative Activities Grants Program and the Donors of the Petroleum Research Fund, administered by the American Chemical Society, is gratefully acknowledged. Pulse radiolysis and flash photolysis were performed at the Center for Fast Kinetics Research, supported by NIH (RR 00886) and by the University of Texas at Austin. I would like to thank J. Maticic, M. Rubin, P. Glaser, and B. Smith for technical assistance, Professor R. M. Bullock for performing the γ-radiolysis experiment, and Professor D. H. R. Barton for helpful comments.

Registry No. $CH_3OCOC_6H_5^{\bullet-}$, 34533-12-5; $CH_3CH_2OCOC_6H_5^{\bullet-}$, 34533-19-2; $(CH_3)_3CCH_2OCOC_6H_5^{\bullet-}$, 123412-28-2; $(CH_3)_2CHOCOC_6H_5^{\bullet-}$, 34533-20-5; $(CH_3)_3COCOC_6H_5^{\bullet-}$, 92344-51-9; $HC{\equiv}CC(CH_3)_2OCOC_6H_5^{\bullet-}$, 123412-29-3; $C_6H_5CH_2OCOC_6H_5^{\bullet-}$, 115116-44-4; p-$CH_3OC_6H_4CH_2OCOC_6H_5^{\bullet-}$, 123412-30-6; $C_6H_5CH(CH_3)OCOC_6H_5^{\bullet-}$, 123484-47-9; $(C_6H_5)_2CHOCOC_6H_5^{\bullet-}$, 115077-09-3; $(C_6H_5)_2C(CH_3)OCOC_6H_5^{\bullet-}$, 123412-31-7; C_6H_7-o-$(COOCH_2CH_3)_2^{\bullet-}$, 34537-32-1; $C_6H_5COOCOC_6H_5^{\bullet-}$, 69209-67-2; $C_6H_5CH_2OCOCH_3^{\bullet-}$, 115116-45-5; $(C_6H_5)_2CHOCOCH_3^{\bullet-}$, 115077-10-6; $CH_3CHO^{\bullet-}$, 60427-04-5; $CH_3OCOC_6H_5$, 93-58-3; $(CH_3)_3CCH_2OCOC_6H_5$, 3581-70-2; $(CH_3)_2CHOCOC_6H_5$, 939-48-0; $(CH_3)_3COCOC_6H_5$, 774-65-2; $HC{\equiv}CC(CH_3)_2OCOC_6H_5$, 56438-73-4; $C_6H_5CH_2OCOC_6H_5$, 120-51-4; p-$CH_3OC_6H_4CH_2OCOC_6H_5$, 24318-41-0; $C_6H_5CH(CH_3)OCOC_6H_5$, 13358-49-1; $(C_6H_5)_2CHOCOC_6H_5$, 7515-28-8; $(C_6H_5)_2C(CH_3)OCOC_6H_5$, 24318-53-4; C_6H_4-o-$(COOCH_2CH_3)_2$, 84-66-2; $C_6H_5COOCOC_6H_5$, 93-97-0; $C_6H_5CH_2OCOCH_3$, 140-11-4; $(C_6H_5)_2CHOCOCH_3$, 954-67-6; $CH_3CH_2OCOC_6H_5$, 93-89-0; benzyl radical, 2154-56-5; diphenylmethyl radical, 4471-17-4; benzophenone, 119-61-9.

Bioactive Peptides: Solid-State and Solution Conformation of Cyclolinopeptide A

Benedetto Di Blasio,[†] Filomena Rossi,[†] Ettore Benedetti,[†] Vincenzo Pavone,[†] Carlo Pedone,[†] Piero Andrea Temussi,[†] Giancarlo Zanotti,[‡] and Teodorico Tancredi*[,§]

Contribution from the Dipartimento di Chimica, Universita' di Napoli, Via Mezzocannone, 4 80134 Napoli, Italy, Centro di Chimica del Farmaco del CNR, Universita' di Roma "La Sapienza", Roma, Italy, and Istituto Chimica MIB del CNR, Via Toiano 6, 80072 Arco Felice, Italy. *Received January 24, 1989*

Abstract: The solid-state and solution conformational analysis of cyclolinopeptide A, a cyclic nonapeptide isolated from linseed, is reported. The X-ray crystal structure determination of the orthorhombic form obtained from a 2-propanol–water mixture [a = 32.98 (3) Å, b = 21.65 (2) Å, c = 9.83 (1) Å, space group $P2_12_12_1$, Z = 4] shows the presence of five strong transannular intramolecular hydrogen bonds with the formation of one C_7, two C_{10} (one type I and one type III), one C_{13}, and one C_{17} ring structures. One peptide unit (linking residues Pro^1 and Pro^2) is cis (ω = 10°); all others are trans. The results of the conformational study in solution by NMR spectroscopy indicate that, provided one choses the right environment, solid-state and solution conformations are essentially identical, even if this cyclic system tends to give rise to a complex mixture of quasi-isoenergetic conformations, favored by the flexibility of the ring enhanced by the isomerism of the Pro–Pro bond and by polar solvents.

Cyclolinopeptide A (henceforth called CLA) is a cyclic nonapeptide of the following sequence:

cyclo-(Pro-Pro-Phe-Phe-Leu-Ile-Ile-Leu-Val)

It has been isolated from linseed[1] and subsequently synthesized by Prox and Weigand[2] by classical solution methods. Soon after its synthesis it has been the object of intensive structural studies[3-5] mainly because it is one of the first isolated natural cyclic peptides and also because the presence of two Pro residues suggests that the accessible conformational space might be limited with respect to those of known medium-sized peptides.

Neither the CD[3] nor NMR[4] studies (in spite of the assignment of the resonances in DMSO-d_6 to residue types[4,6]) have given an

* To whom correspondence should be addressed.

(1) Kaufmann, H. P.; Tobschirbel, A. *Chem. Ber.* **1959**, *92*, 2805–2809.
(2) Prox, A.; Weygand, F. In *Peptides. Proceedings of the 8th European Peptide Symposium*; Beyerman, H. C.; van de Linde, A.; Maasen van den Brink, W., Eds.; Elvesier/North-Holland Biomedical Press: Amsterdam and New York, 1966; pp 158–172.
(3) Naider, F.; Benedetti, E.; Goodman, M. *Proc. Natl. Acad. Sci. U.S.A.* **1971**, *68*, 1195–1198.
(4) Brewster, A. I.; Bovey, F. A. *Proc. Natl. Acad. Sci. U.S.A.* **1971**, *68*, 1199–1202.
(5) Tonelli, A. E. *Proc. Natl. Acad. Sci. U.S.A.* **1971**, *68*, 1203–1207.

0002-7863/89/1511-9089$01.50/0

Table I. Crystallographic Data for Cyclolinopeptide A

molecular formula	$C_{57}H_{85}N_9O_9 \cdot 2(CH_3)_2CHOH \cdot H_2O$
molecular weight, amu	1178.6
crystal system	orthorhombic
space group	$P2_12_12_1$
Z, molecules/unit cell	4
a, Å	32.98 (3)
b, Å	21.65 (2)
c, Å	9.83 (1)
V, Å^3	7018.8
d_{calc}, g/cm	1.115
d_{exptl}, g/cm	1.11
radiation, Å	Cu Kα (λ = 1.5418)
measured reflections	3389
reflections with $I > 3.0\sigma(I)$	2942
final R value	0.082
temp, °C	23, ambient

understandable picture of the conformation in solution.

The difficulty of finding a single conformation consistent with spectral parameters may be linked to the flexibility of this cyclic peptide, comparable to that of linear peptides. In fact, the presence of Pro residues, although effective in reducing the accessible conformational space, does not prevent the existence of a number of conformers that is large with respect to the number of experimental data in solution.

Interest in solving the structure of this peptide has been greatly rekindled by the discovery that it is endowed with a remarkable cytoprotective ability.[7] In particular, it is able to inhibit the uptake of cholate by hepatocytes.

It was also shown[6] that this biological activity is linked to well-defined sequential features shared by another natural cyclic peptide, i.e., antamanide,[8] and by several analogues[9] (Pro-Pro-Phe-Phe moiety).

Although the mechanism of action has not yet been elucidated, it is clear that the biological activity is critically dependent upon the sequence and conformation of the peptide.[9] It seems interesting to try to establish the conformation–activity relationship, also with respect to the conformational features already found[9] for other cytoprotective peptides. The conformation, in turn, may be influenced by the nature of the biological environment. Thus, in order to formulate more detailed proposals on the mechanism of action of CLA, it is essential to study its conformation in several environments with different physicochemical characteristics.

Here we present a full conformational analysis of CLA in the solid state and in solution of several media, in a wide temperature range.

Experimental Section

CLA was prepared as described in ref. 10. It was purified by crystallization from 2-propanol–water mixtures.

Solid-State Conformational Study. (A) X-ray Data Collection. Colorless crystals, in the form of small needles, were obtained by slow evaporation at room temperature of 2-propanol–water solutions. A crystal, 0.20 × 0.30 × 0.08 mm in size, was used for the unit-cell determination and intensity data collection. Preliminary oscillation and Weissenberg photographs were taken to establish the crystal symmetry and the space group. The determination of the lattice constants and the collection of the X-ray intensity data were performed on a Picker four-circle automated diffractometer equipped with a PDP-8 Digital computer at the former Polytechnic Institute of Brooklyn, now Polytechnic Institute of New York. The cell dimensions, given in Table I together with other relevant crystal data, were determined from a least-squares treatment of the setting angles of 20 reflections with high values of 2θ. Integrated intensities were measured by the $\theta - 2\theta$ scan mode using Ni-filtered Cu Kα radiation (λ = 1.5418 Å) and pulse height analysis to reduce unwanted background. A scan range of 1.5° was found to be sufficient for all the reflections over the range of 2θ examined (0–130°) with a scan speed of 1°/mm. The counter aperture, 4.0 × 4.0 mm was placed 30 cm from the crystal. Two stationary crystal – stationary counter background counts of 10 s were taken at each end of each scan.

A total of 3389 independent reflections were collected, 2942 of which, having $I > 3.0\sigma(I)$, were considered observed. Two standard reflections were measured every 25 reflections during data collection (approximately every 60 min) to check the electronic stability of the instrument and any deterioration of the crystal. The fluctuations in the intensities of the standard reflections were within 3% of their intensities. The integrated intensities, from which the background counts were subtracted, were then corrected for Lorentz and polarization effects.

The calculated density, based on four units per cell (Z = 4), constituted by one cyclopeptide molecule of formula $C_{57}H_{85}N_9O_9$, two 2-propanol molecules, and one water molecule, is 1.115 g/cm^3, in good agreement with the experimental density of 1.11 g/cm^3, measured by flotation techniques in n-hexane–chloroform mixtures.

(B) Structure Determination and Refinement. Many attempts to solve the phase problem of the cyclic nonapeptide by direct methods, using different phase determination procedures as programmed in various crystallographic computing programs (MULTAN, RANTAN, YZARC, MAGEX), did not yield the solution of the crystal structure.

We then proceeded to apply the molecular replacement technique by using a molecular fragment of known structure as a starting model, which eventually gave the solution of the structure. The starting model for the vector search procedure was partially derived from a model recently proposed by Kessler et al.,[7] on the basis of NMR studies of a series of peptides presenting similar cytoprotective activity. In fact, the similarity of conformation shown in solution by the Pro-Pro-Phe sequence, which is common to those of both cyclolinopeptide A and antamanide, even in different solvent systems, has prompted us to use the structure of this fragment, obtained from the known structure of natural antamanide,[11] as a starting model.

This model fragment, containing a total of 25 atoms, was used for the search in the Patterson map of the CLA molecule computed with EF coefficients, where the F and E values are the experimentally measured structure factors and the corresponding normalized values, respectively. The subsequent translation search placed the oriented model correctly with respect to an origin of the unit cell. For this procedure, the computer program PATSEE, as included in the SHELX84 program package,[12] was used. Completion of the structure of the cyclic peptide was eventually obtained from the 25-atom fragment by the partial structure procedure of SHELX84 and difference Fourier maps. In these maps the presence of two 2-propanol and one water molecules for each peptide molecule was also revealed.

Full-matrix least-squares refinement,[13] initially with isotropic thermal factors and subsequently with anisotropic thermal factors for the C, N, and O atoms, gave an overall agreement factor of R = 0.082 for 2942 reflections with $I > 3\sigma(I)$. The position of the oxygen atom of the water molecule, which is involved in strong hydrogen bonds with the peptide molecule, has been univocally determined and well refined. On the contrary, the position of the atoms of the two independent 2-propanol solvent molecules is not well defined. In fact, although the oxygen atoms of the two 2-propanol molecules participate in hydrogen bonds, these solvent molecules occur in a large cavity, which allows them to assume a disordered position.

Hydrogen atoms were introduced in their stereochemically expected positions with isotropic temperature factors equal to the equivalent U factor of the atom to which each of them is linked. Refinement was ended when the shifts in the atomic coordinates and anisotropic temperature factors for the heavy atoms were less than $^1/_5$ and $^1/_3$ of the corresponding standard deviations, respectively. In Table II the final fractional coordinates and thermal parameters for the refined atoms are reported.

Solution Conformational Analysis. ^{1}H NMR spectra were recorded on Bruker spectrometers (AC 270, AM 400, and WM 500) and processed on a Bruker data station with an Aspect 1000 computer and a 160-Mbytes disk.

A 0.5-mL amount of 6 mM CLA in 5-mm tubes (Wilmad, Buena, NJ) was used for all samples in different solvents. DMSO·d_6 (99.96%

(6) Siemion, I. Z.; Klis, W. A.; Sucharda-Sobczyk, A.; Obermeier, R. *Rocniki Chem.* **1977**, *51*, 1489–1498.
(7) Kessler, H.; Kelin, M.; Muller, A.; Wagner, K.; Bats, J. W.; Ziegler, K.; Frimmer, M. *Angew. Chem., Int. Ed. Engl.* **1986**, *25*, 997–999.
(8) Wieland, T. In *Chemistry and Biology of Peptides*; Meienhofer, J., Ed.; Ann Arbor Science: Ann Arbor, MI, 1972; pp 377–396.
(9) Kessler, H.; Bats, J. W.; Griesinger, C.; Koll, S.; Will, M.; Wagner, K. *J. Am. Chem. Soc.* **1986**, *110*, 1033–1049.
(10) Tancredi, T.; Zanotti, G.; Rossi, F.; Benedetti, E.; Pedone, C.; Temussi, P. A. *Biopolymers* **1989**, *28*, 513–523.
(11) Karle, I. L.; Wieland, T.; Schermer, D.; Ottenheym, H. C. J. *Proc. Natl. Acad. Sci. U.S.A.* **1979**, *76*, 1532–1536.
(12) Egert, E.; Sheldrick, G. M. *Acta Crystallogr. Sect. A* **1985**, *41*, 262–268.
(13) Sheldrick, G. M. *SHELX 76: Programs for Crystal Structure Determination*; University of Cambridge, England, 1975.

Table II. Final Atomic Parameters and Their Standard Deviations (in Parentheses) for CLA

	X/A	*Y/B*	*Z/C*	*U*		*X/A*	*Y/B*	*Z/C*	*U*
N_1	.1085 (3)	0.9264 (4)	0.2501 (8)	0.058	C'_5	−0.0308 (3)	0.9447 (5)	−0.1599 (12)	0.070
C_1^{α}	0.1430 (3)	0.9523 (5)	0.1751 (10)	0.055	O_5	−0.0531 (3)	0.9704 (4)	−0.0742 (9)	0.078
C_1^{β}	0.1469 (4)	1.0195 (6)	0.2330 (12)	0.081	N_5	−0.0435 (3)	0.9027 (4)	−0.2516 (8)	0.069
C_1^{γ}	0.1303 (4)	1.0128 (6)	0.3736 (13)	0.084	C_6^{α}	−0.0861 (3)	0.8865 (6)	−0.2639 (12)	0.083
C_1^{δ}	0.0963 (4)	0.9674 (5)	0.3595 (12)	0.074	C_6^{β}	−0.0871 (5)	0.8341 (8)	−0.3692 (13)	0.110
C'_1	0.1813 (3)	0.9148 (6)	0.1956 (13)	0.069	C_6^{δ}	−0.1573 (6)	0.8633 (14)	−0.4577 (29)	0.264
O_1	0.1855 (3)	0.8803 (4)	0.2954 (9)	0.084	$C_6^{\gamma 2}$	−0.0630 (6)	0.7763 (7)	−0.3351 (16)	0.134
N_2	0.2114 (3)	0.9213 (4)	0.1034 (10)	0.066	$C_6^{\gamma 1}$	−0.1296 (7)	0.8114 (12)	−0.4018 (21)	0.196
C_2^{α}	0.2136 (3)	0.9681 (5)	−0.0045 (12)	0.073	C'_6	−0.1032 (4)	0.8652 (6)	−0.1260 (12)	0.079
C_2^{β}	0.2584 (4)	0.9768 (7)	−0.0215 (16)	0.096	O_6	−0.1399 (3)	0.8725 (5)	−0.1076 (9)	0.107
C_2^{γ}	0.2782 (4)	0.9152 (8)	0.0085 (18)	0.108	N_7	−0.0786 (3)	0.8357 (5)	−0.0417 (8)	0.064
C_2^{δ}	0.2510 (4)	0.8920 (7)	0.1250 (15)	0.091	C_7^{α}	−0.0923 (4)	0.8145 (6)	0.0916 (10)	0.074
C'_2	0.1942 (4)	0.9468 (6)	−0.1376 (12)	0.069	C_7^{β}	−0.0906 (4)	0.7441 (6)	0.1068 (13)	0.090
O_2	0.1862 (3)	0.9877 (5)	−0.2209 (11)	0.108	$C_7^{\gamma 1}$	−0.0481 (4)	0.7175 (6)	0.0870 (15)	0.091
N_3	0.1867 (3)	0.8874 (4)	−0.1643 (9)	0.063	$C_7^{\gamma 2}$	−0.1211 (5)	0.7120 (6)	0.0123 (15)	0.112
C_3^{α}	0.1708 (3)	0.8660 (5)	−0.2927 (11)	0.063	C_7^{δ}	−0.0416 (6)	0.6532 (7)	0.1439 (23)	0.187
C_3^{β}	0.1921 (3)	0.8063 (5)	−0.3379 (12)	0.065	C'_7	−0.0706 (4)	0.8477 (6)	0.2063 (11)	0.071
C_3^{γ}	0.2379 (4)	0.8120 (6)	−0.3579 (14)	0.073	O_7	−0.0690 (3)	0.8247 (4)	0.3211 (8)	0.082
$C_3^{\delta 1}$	0.2519 (5)	0.8511 (7)	−0.4593 (15)	0.096	N_8	−0.0534 (3)	0.9026 (5)	0.1797 (9)	0.071
$C_3^{\varepsilon 1}$	0.2938 (5)	0.8542 (7)	−0.4810 (17)	0.105	C_8^{α}	−0.0338 (3)	0.9423 (5)	0.2810 (8)	0.068
C_3^{ζ}	0.3202 (5)	0.8217 (9)	−0.3993 (21)	0.119	C_8^{β}	−0.0635 (4)	0.9694 (6)	0.3809 (12)	0.078
$C_3^{\eta 2}$	0.3056 (5)	0.7847 (11)	−0.2975 (22)	0.165	C_8^{γ}	−0.0901 (6)	1.0182 (10)	0.3147 (22)	0.176
$C_3^{\delta 2}$	0.2644 (5)	0.7792 (7)	−0.2746 (15)	0.098	$C_8^{\delta 1}$	−0.0672 (9)	1.0722 (12)	0.2643 (40)	0.327
C'_3	0.1246 (3)	0.8569 (6)	−0.2863 (12)	0.069	$C_8^{\delta 2}$	−0.1207 (8)	1.0392 (10)	0.4174 (26)	0.238
O_3	0.1040 (3)	0.8738 (4)	−0.3813 (8)	0.081	C'_8	−0.0008 (4)	0.9052 (6)	0.3549 (13)	0.079
N_4	0.1091 (3)	0.8250 (4)	−0.1817 (9)	0.061	O_8	0.0063 (3)	0.9090 (4)	0.4791 (8)	0.086
C_4^{α}	0.0673 (3)	0.8028 (5)	−0.1805 (11)	0.060	N_8	0.0245 (3)	0.8736 (4)	0.2729 (9)	0.055
C_4^{β}	0.0642 (4)	0.7405 (5)	−0.1026 (13)	0.077	C_9^{α}	0.0613 (3)	0.8442 (5)	0.3162 (10)	0.059
C_4^{γ}	0.0834 (5)	0.6897 (5)	−0.1811 (14)	0.078	C_9^{β}	0.0608 (4)	0.7735 (4)	0.3130 (12)	0.070
$C_4^{\delta 1}$	0.1230 (5)	0.6721 (8)	−0.1688 (20)	0.121	$C_9^{\gamma 1}$	0.1008 (4)	0.7470 (7)	0.3648 (15)	0.102
$C_4^{\varepsilon 1}$	0.1394 (6)	0.6256 (8)	−0.2498 (23)	0.149	$C_9^{\gamma 2}$	0.0248 (4)	0.7506 (7)	0.3994 (13)	0.101
C_4^{ζ}	0.1150 (6)	0.5971 (8)	−0.3413 (20)	0.131	C'_9	0.0959 (3)	0.8701 (4)	0.2252 (11)	0.056
$C_4^{\eta 2}$	0.0752 (6)	0.6133 (9)	−0.3544 (19)	0.131	O_9	0.1086 (2)	0.8407 (4)	0.1274 (8)	0.079
$C_4^{\delta 2}$	0.0593 (5)	0.6607 (7)	−0.2775 (17)	0.111	O_w	0.1787 (2)	0.7818 (3)	0.0185 (8)	0.085
C'_4	0.0387 (3)	0.8535 (5)	−0.1266 (10)	0.057	O_{11}	0.2099 (4)	0.3691 (7)	0.4649 (16)	0.194
O_4	0.0170 (2)	0.8443 (4)	−0.0257 (8)	0.067	C_{11}	0.2070 (8)	0.4246 (15)	0.3668 (36)	0.294
N_5	0.0396 (3)	0.9064 (4)	−0.1925 (9)	0.063	C_{12}	0.2206 (18)	0.4647 (16)	0.4798 (43)	0.395
C_5^{α}	0.0146 (4)	0.9580 (4)	−0.1522 (11)	0.064	C_{13}	0.2429 (15)	0.4185 (19)	0.3036 (43)	0.387
C_5^{β}	0.0246 (4)	1.0167 (6)	−0.2340 (13)	0.086	O_{12}	0.2683 (5)	0.3049 (8)	0.6100 (18)	0.223
C_5^{γ}	0.0692 (6)	1.0367 (9)	−0.2042 (24)	0.156	C_{11b}	0.2821 (8)	0.3185 (18)	0.7572 (28)	0.341
$C_5^{\delta 1}$	0.0692 (9)	1.0669 (12)	−0.0647 (27)	0.277	C_{12b}	0.2485 (10)	0.2763 (15)	0.8044 (37)	0.302
$C_5^{\delta 2}$	0.0789 (8)	1.0921 (11)	−0.2913 (28)	0.221	C_{13b}	0.2747 (14)	0.3695 (16)	0.8569 (66)	0.596

^{2}H atom) and $CDCl_3$ (99.98% ^{2}H atom) were purchased from Aldrich (Milwakee, WI). D_2O (99.98%) and CD_3OH (99.8% ^{2}H atom) were purchased from C. Erba (Milano, Italy), and $(CD_3)_2CDOH$ (99% ^{2}H atom) was purchased from Sigma (St. Louis, MO). All chemical shifts are referred to internal tetramethylsilane (TMS). In one-dimensional (1D) spectra, 32–80 scans were acquired, with 16K or 32K sizes for acquisition and 32K or 64K, respectively, for transformation; a Lorentz to Gauss[14] multiplication was used for resolution enhancement (typically, LB = −3 and GB = 0.1). The temperatures were accurate within ±1 deg. Pulse programs of the standard Bruker software library were used for two-dimensional (2D) experiments. All 2D spectra were run at 214 K.

(A) DQF COSY (500 MHz). A total of 512 experiments of 80 scans each were performed: relaxation delay, 1 s; size, 2K; 6024-Hz spectral width in F_2; zero filling to 4K in F_2 and 1K in F_1; apodization in both dimensions with Lorentz to Gauss multiplication (GB = 0.08; LB = −3). The spectrum was acquired in the phase-sensitive mode, with quadrature detection in both dimensions, by use of the time proportional phase increment (TPPI).[15]

(B) HOHAHA (400 MHz). The phase-sensitive spectrum was performed in the low-power transmitter mode. The 90° flip angle was 70 μs, and the total mixing time was 74 ms. A total of 256 experiments of 80 scans each were performed: relaxation delay, 1 s; spectral width, 4000 Hz in F_2; size, 2K; zero filling to 4K in F_2 and 1K in F_1; apodization in both dimensions with squared cosine windows.

(C) DQ (500 MHz). A total of 256 experiments of 160 scans each were performed: relaxation delay, 1 s; D_2 = 7.8 ms; size, 2K; spectral width, 6024 Hz in F_2; zero filling to 4K in F_2 and 1K in F_1; apodization in both dimensions with squared cosine windows.

(D) NOESY (500 MHz). The spectra were performed in the phase-sensitive mode: 416 experiments of 80 scans each; relaxation delay, 1 s; size, 2K; spectral width, 6024 Hz in F_2; zero filling to 4K in F_2 and 1K in F_1; mixing time, 350 ms with 10% random variation; Lorentz to Gauss multiplication in both dimensions (GB = 0.08; LB = −3).

Results and Discussion

Solid-State Structure and Conformation. The molecular model of CLA, as derived from the crystal structure analysis, is shown in Figure 1, while Figure 2 gives a stereoview in a direction almost perpendicular to the average plane of the cyclic molecule. All the amino acid residues are in the L configuration. The observed bond lengths and bond angles are near the expected values[16] and should be considered unexceptional. The nonapeptide presents in the backbone eight trans peptide bonds and one cis peptide bond (ω = 10°) occurring between the two proline (Pro^1-Pro^2) residues. The range of values for the trans peptide bonds is 167–179°, with an average value of 175°.

(14) Ernst, R. R. *Adv. Magn. Reson.* **1966**, *2*, 1–135.
(15) Marion, D.; Wuthrich, K. *Biochim. Biophys. Res. Commun.* **1983**, *113*, 967–974.
(16) Benedetti, E. *Chemistry and Biochemistry of Amino Acids, Peptides and Proteins*; Weinstein, B., Ed.; Marcel Dekker: New York, 1982; Vol. 6, pp 105–184.

Table III. Hydrogen Bonds

type	donor	acceptor	length, Å	angle, deg (N–H···O)
intramolecular				
C13	N(4)	O(9)	3.06	122
C7	N(5)	O(3)	2.91	145
C10	N(7)	O(4)	3.16	145
C10	N(8)	O(5)	2.89	162
C17	N(9)	O(4)	3.01	161
intermolecular	N(6)	O(8) (x, y, $-z$)	3.12	132
peptide–solvent	N(3)	O(w)	2.92	
	O(w)	O(9)	2.85	
	O(I1) ($-x$, $^1/_2 + y$, $^1/_2 - z$)	O(6)	2.71	
solvent–solvent	O(I2)	O(I1)	2.82	
	O(w)	O(I2) ($^1/_2 - x$, $1 - y$, $z - ^1/_2$)	2.72	

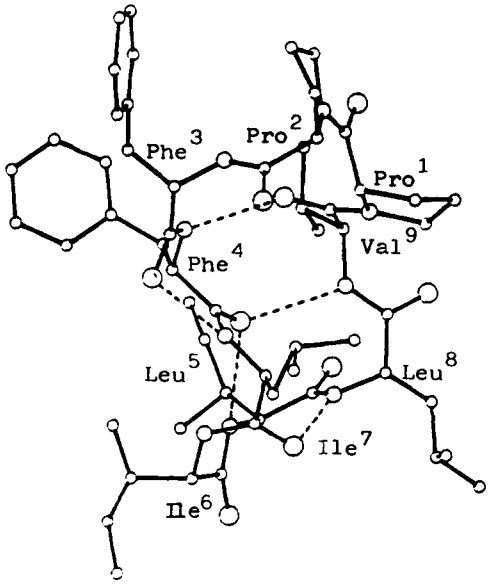

Figure 1. Molecular model of CLA. The numbering of each residue is reported. Intramolecular hydrogen bonds are indicated as dashed lines.

The conformation of uncomplexed cyclic peptides is frequently stabilized by internal transannular NH···O=C hydrogen bonds of the 3 → 1 (γ-turn), 4 → 1 (β-turn), and/or 5 → 1 (α-turn) types, depending upon the size of the ring and conformation of the backbone. These types of intramolecular hydrogen bond are also seen in the crystal structure of CLA. Details on intramolecular and intermolecular hydrogen bonds are reported in Table III. The backbone conformation of CLA is stabilized in the solid state by the following bonds:

(i) An intramolecular 3 → 1 (γ-turn) H-bond involving the N–H of Leu^5 and the C=O of Phe^3.

(ii) Two consecutive 4 → 1 (β-turn) H-bonds: one of type III, between the NH of Ile^7 and the C=O of Phe^4, and one of type I, between the NH of Leu^8 and the C=O of Leu^5.

(iii) An intramolecular 5 → 1 (α-turn) H-bond involving the NH of Phe^4 and the C=O of Val^9. Internal to this cyclic H-bonded structure, the cis peptide unit (between Pro^1 and Pro^2) is contained.

(iv) A C_{17} ring structure stabilized by an intramolecular hydrogen bond between the NH of Val^9 and the C=O of Phe^4. This hydrogen bond can also be considered a C_{16} ring structure counting the atoms of the ring formed by the remaining portion of the cyclic molecule.

The conformation of the backbone and side chains for each residue is best described by the conformational parameters given in Table IV. All values for the pairs φ, ψ fall within the allowed regions for L residues except for Leu^8 which presents values of $\varphi = 55°$, $\psi = 48°$ appreciably higher in energy, corresponding to the left-handed helical region. However, in this conformation this residue is able to form two hydrogen bonds of the NH···O=C type, one with its NH group (intramolecularly with the C=O of Leu^5) and one with its C=O group (intermolecularly with the NH of Ile^6).

The conformational parameters of the Pro-Pro-Phe peptide sequence have striking similarity with those of the homologue sequence of the natural cyclic decapeptide antamanide,[11] with differences that on the average are not greater than 22°. A substantial difference is present in the conformation of the Phe^4 residue of the two cyclic molecules, since the φ and ψ values are −88°, 59° and 70°, 30° for CLA and antamanide, respectively.

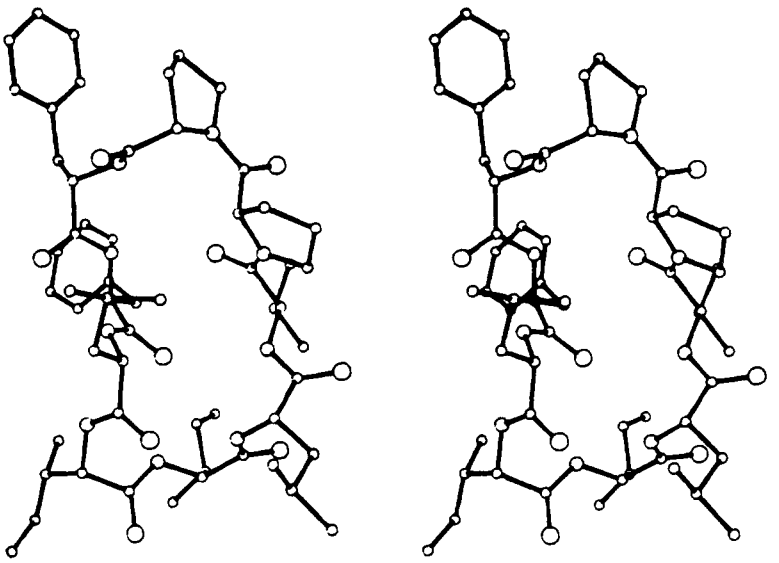

Figure 2. Stereoview of the CLA molecule in a direction almost perpendicular to the average plane of the 27-incartered ring.

Table IV. Conformational Parameters for Cyclolinopeptide A[a]

angle, deg[b]	Pro[1]	Pro[2]	Phe[3]	Phe[4]	Leu[5]	Ile[6]	Ile[7]	Leu[8]	Val[9]
φ_i	−60.0	−90.3	−97.3	−86.0	−61.5	−55.2	−114.7	55.1	−125.0
ψ_i	160.2	−17.7	−48.7	56.7	−28.2	−32.7	21.5	48.4	74.8
ω_i	10.0	−175.9	−166.9	−179.5	178.9	179.4	175.6	169.2	175.5
$\chi_i^{1,1}$	28.1	32.2	−60.1	−70.7	−63.1	−177.9	59.2	−71.0	−178.3
$\chi_i^{1,2}$						59.4	−66.6		−55.8
$\chi_i^{2,1}$			−63.9	91.4	176.9	58.8	161.1	175.7	
$\chi_i^{2,2}$			115.2	−85.5	−76.4			−62.9	

[a] The torsion angles for rotation about bonds of the peptide backbone and about bonds of the amino acid side chains are described in IUPAC–IUB, Commission on Biochemical Nomenclature *Biochemistry* **1970**, *9*, 3471–3479. [b] Estimated esd ≈ 1.1°.

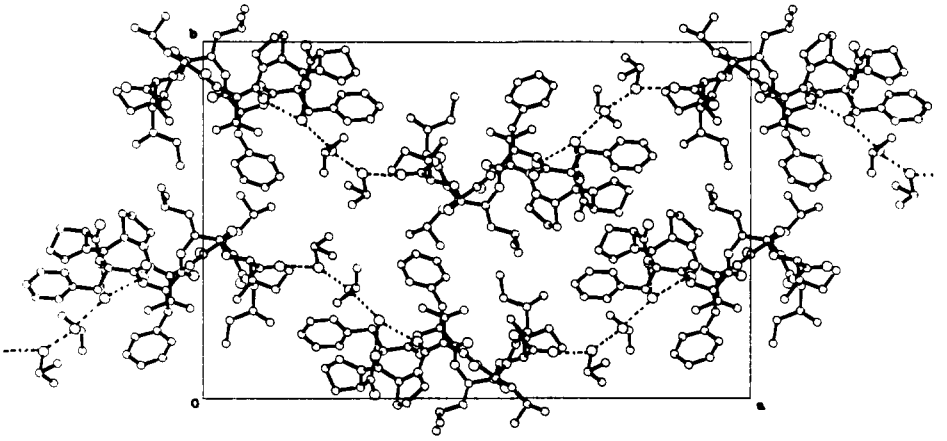

Figure 3. Mode of packing of the CLA molecules as view along the *c* axis. Intramolecular hydrogen bonds between peptide and solvent molecules are indicated as dashed lines. The peptide to peptide intermolecular hydrogen bond of the N—H···O=C type occurring along the *c* axis is not shown.

It is interesting to note that the Phe[5] and Phe[10] residues of antamanide have a similar φ and ψ values (identical for Phe[10]) to those of Leu[8] of the present structure.

The conformation of the side chains for each residue is very close to one of those more often observed in peptides[17]. In fact, for example, the Phe side chains have χ^1 and χ^2 values close to −60° (g^- conformation) and 90°, respectively; the conformation of the two Leu side chains can be described as g^- (t, g^-), one of the more frequently observed conformations in peptides, and finally, the side chain conformations of the Val (t, g^- conformation for the $\chi_9^{1,1}$ and $\chi_9^{1,2}$ angles) and of the two Ile residues (t, g^+ and g^+, g^- conformations for the pairs of $\chi_6^{1,1}$, $\chi_6^{1,2}$ and $\chi_7^{1,1}$, $\chi_7^{1,2}$ angles, respectively) also are close to the conformations more commonly observed for these residues.[17] The side-chain conformation of the two prolyl residues is of the C^γ-endo type, being characterized by positive χ^1 and χ^3 values and negative χ^2 and χ^4 values. A further similarity between CLA and antamanide structures regards the Pro[2]-Phe[3] side-chain conformation. It is possible to observe a stacking of the rings of these two residues that is similar to those occurring in all antamanide structures and in other peptides containing the Pro-Phe sequence.

The molecules in the solid state are held together by a network of hydrogen bonds as described in Table III and Figure 3. All H-bond donors are involved in the H-bond scheme. All distances of the type N–H···O and O–H···O are within expected values.[18] Two NH groups are intermolecularly H-bonded: as already mentioned, the NH of Ile[6] is bonded to the C=O group of the Val[9] residue of a molecule translated along the *z* axis, while the NH group of Phe[3] is H-bonded to the oxygen atom of the water molecule. The water molecule on the other hand acts as a H-bond donor with respect to both the C=O group of Val[9] and the C–OH group of one of the 2-propanol solvent molecules.

The 2-propanol molecule accepting the H-bond from the water molecule acts as a donor with respect to the second 2-propanol molecule, which in turn acts as a donor with respect to the C=O group of Ile.[6] The three independent solvent molecules fill a channel in the solid state in the *c* direction, bridging molecules of CLA in a layer perpendicular to the *b* axis. In fact, along the *a* direction the CLA molecules are held together in the crystal by hydrogen bonds with the solvent molecules, while in the *c* direction they are directly connected through hydrogen bonds. Consequently, a layer of CLA and solvent molecules, almost parallel to the *ac* plane, is seen. In the other direction (*b* axis) these layers of CLA and solvent molecules are held together by van der Waals contacts between interacting side-chain hydrophobic groups.

Solution Conformational Analysis. The preliminary NMR data that appeared in the literature,[4,6] notably the temperature and field dependence of the spectra, indicated that indeed the room- and high-temperature spectra of CLA in polar solvents stem from a mixture of several conformers in intermediate and fast chemical exchange, respectively. Although NMR spectroscopy is now well established as the major technique for conformational analysis of peptides in solution,[19] it is very difficult to extract conformational parameters from a mixture of two or more conformers in rapid equilibrium.[20] The presence of more than one conformer is to be expected, in particular when Pro residues are present, since each Pro may give rise to families of conformations characterized by a cis or trans Xxx–Pro bond, respectively. It is the aim of this study to find experimental conditions that can reduce the number of conformers in equilibrium and/or slow down the rate of interconversion. Accordingly, we present a ^{1}H NMR study of CLA in several solvent media of different polarity at different magnetic fields and in a wide temperature range.

(A) NMR Spectra in Polar Solvents. The room-temperature ^{1}H spectrum of 6 mM CLA in DMSO-d_6 at 270 MHz is characterized by very broad backbone proton resonances, notably those of the amide protons. Increasing the field strength to 400 or 500

(17) Benedetti, E.; Morelli, G.; Nemethy, G.; Scheraga, H. A. *Int. J. Pept. Protein Res.* **1983**, *22*, 1–15.

(18) Ramakrishanan, C.; Prasad, N. *Int. J. Pept. Protein Res.* **1971**, *3*, 209–231.

(19) Kessler, H.; Bermel, W.; Muller, A.; Pook, K. H. In *The Peptides*; Underfriend, S.; Meienhofer, J., Eds.; Academic Press: London, 1985; Vol. 7, pp 438–473.

(20) Temussi, P. A.; Picone, D.; Castiglione-Morelli, M. A.; Motta, A.; Tancredi, T. *Biopolymers* **1989**, *28*, 91–107.

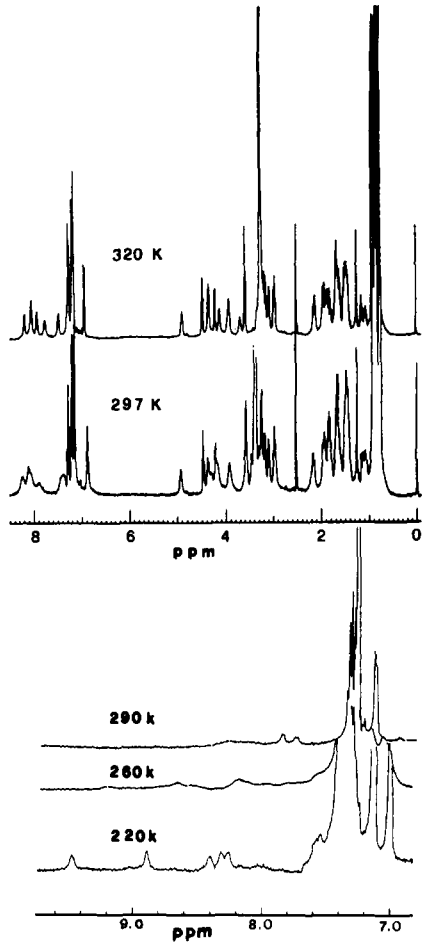

Figure 4. (Above) 500-MHz ^1H NMR spectra of 6 mM CLA in DMSO-d_6 at room and high temperature; (below) low-field region of the 400-MHz ^1H NMR spectra of 6 mM CLA in a 70/30 (v/v) DMSO/H_2O mixture, in the 220–290 K temperature range.

MHz results in an even more pronounced broadening of such resonances, leaving fairly well resolved peaks only for the side-chain protons. A control spectrum of 0.6 mM CLA in the same solvent confirmed such a behavior, hence ruling out aggregation phenomena as the cause of the broadening.

The results are indicative of the existence, in solution, of several conformers in intermediate chemical exchange. Increasing the temperature to 320 K and above gives rise to spectra with well-resolved, sharp resonances throughout; Figure 4 shows a comparison of the 500-MHz spectra of 6 mM CLA in DMSO-d_6 at room and high temperature. The usefulness of interpreting the high-temperature spectrum in terms of conformational parameters is questionable. In fact, we are probably looking at coalesced peaks, resulting from fast exchange among quasi-isoenergetic conformers, and there is no way of assessing whether they originate from a major component. Moreover, all chemical shift values at 320 K correspond closely to those characteristic of unstructured peptides.[21] The absence of outstanding values and the grouping of all NH resonances in a range of only 0.8 ppm, in particular, point to the absence of a single well-defined conformation at this temperature.

Should the hypothesis of chemical exchange among several conformers be correct, the best strategy for "freezing" a single most stable conformational state is to perform NMR experiments at the lowest possible temperature. Owing to its very high melting point, neat DMSO is not a good candidate for low-temperature studies. Among polar solvents we selected three different systems, namely, methanol, 2-propanol, and a DMSO/H_2O mixture. Isopropyl alcohol was choosen alongside methanol because it has intermediate polarity but also because it had been used to obtain the crystal for the X-ray diffraction study. The DMSO/water mixture is one of the so-called cryoprotective mixtures,[22] proposed by Douzou and Petsko for low-temperature studies of proteins. These mixtures are isodielectric with water at very low temperature and possess a fairly high viscosity that changes smoothly as a function of composition and temperature. It has been recently shown that cryoprotective mixtures, contrary to neat DMSO,[23] can be used as structure-inducing media.[24,25] The low-field region of the 400-MHz ^1H spectra of 6 mM CLA in a 70:30 (v/v) DMSO/water mixture at three different temperatures is shown in Figure 4. In the spectrum at 290 K, only the aromatic protons of the two Phe residues and two broad NH peaks are detectable; the remaining amidic resonances are even broader than those in the corresponding spectrum in neat DMSO, merging into the noise. Lowering the temperature to 260 and finally to 220 K causes the appearance of new broad NH resonances that sharpen somewhat and move downfield at the lowest temperature. The increased spread of the chemical shift range of the NH resonances, paralleled by the analogous behavior of the aromatic resonances, suggests the presence, at 220 K, of more structured conformers and/or the reduction of the number of conformers in equilibrium. However, the persistent lack of fine structure and the rapidly changing NH chemical shifts indicate that there is still an equilibrium among several conformers.

The results of the low-temperature studies in methanol and 2-propanol are even less encouraging. We observed once more the appearance, at very low temperatures, of new broad NH peaks, but the quality of the spectra prevents even reliable resonance assignments.

Even the measurement of the temperature coefficients of NH resonances proved possible only for the neat DMSO solution. This widely used parameter may give valuable information on the presence of intramolecular hydrogen bonds, but a reliable interpretation in terms of hydrogen bond is only possible for very low coefficients (e.g., lower than $\approx$ 2 ppb/K) since high values of temperature coefficients may originate both from interactions with the solvent and from the breaking of labile hydrogen bonds.

The values measured for CLA in DMSO solution cannot be interpreted in terms of hydrogen bonds since, in addition to the aforementioned difficulties, they showed a marked dependence on magnetic field strength. Since the normal mechanisms invoked to explain the influence of temperature on NH chemical shifts, i.e., the breakdown of hydrogen bonds and the interactions with solvent molecules, should have a negligible field dependence, it seems reasonable to assume that the temperature coefficients of CLA in DMSO are influenced also by chemical exchange and conformational transitions.

(B) NMR Spectra in Apolar Environment. The most likely cause of the persistence of multiple conformers even at very low temperatures, in polar solvents, is the possibility for CLA to form several different hydrogen bonds with solvent molecules. To prevent this, we resorted to chloroform, a fairly apolar solvent that has the additional advantage of a possible interpretation of high values of temperature coefficients of amidic protons in term of labile intramolecular H-bonds.[26] CLA is very soluble in chloroform; all experiments have been carried out at a concentration of 6 mM CLA, apart from a 10-fold-diluted sample, used to rule out the presence of aggregates.

Figure 5 shows the 500-MHz ^1H spectra of CLA in $CDCl_3$ at three different temperatures. The spectrum at 284 K has very broad resonances, with nearly undetectable NH peaks. Raising

(21) Wuthrich, K. *NMR in Biological Research. Peptides and Proteins*; North-Holland: Amsterdam, 1976.

(22) Duzou, P.; Petsko, G. A. *Adv. Protein Chem.* **1984**, *36*, 245–361.
(23) Bradbury, E. M.; Crane-Robinson, C.; Paolillo, L.; Temussi, P. A. *J. Am. Chem. Soc.* **1973**, *95*, 1683–1684.
(24) Motta, A.; Picone, D.; Tancredi, T.; Temussi, P. A. *Tetrahedron* **1988**, *44*, 975–990.
(25) Fesik, S.; Olejniczak, E. T. *Magn. Reson. Chem.* **1987**, *25*, 1046–1048.
(26) Stevens, E. S.; Sugawara, N.; Bonora, G. M.; Toniolo, C. *J. Am. Chem. Soc.* **1980**, *102*, 7048–7050.

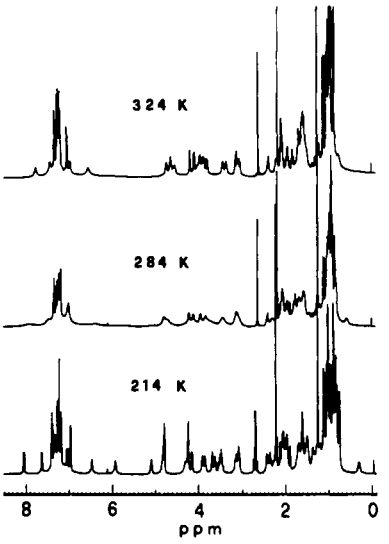

Figure 5. 500-MHz ^1H NMR spectra of 6 mM CLA in $CDCl_3$, in the temperature range 214–324 K.

the temperature to 324 K does induce a sharpening of all resonances, but to a much lesser degree than in the corresponding DMSO spectrum (Figure 4). Lowering the temperature, on the other hand, induces dramatic changes, as can be appreciated from the spectrum at 214 K. The NH peaks are now spread over a range of 2.1 ppm, and a substantial spreading of the aromatic resonances indicates that the two identical Phe side chains are in a different chemical environment. Even more remarkable is the shift to very high field (0.33 ppm) of a single aliphatic peak (assigned to one of the γ protons of a proline residue, vide infra).

These features suggest the existence, in $CDCl_3$ at 214 K, of a single conformer of well-defined structure. We undertook its conformational analysis with the aim of comparing the solution structure with that found in the solid state.

(1) Assignments of NMR Resonances. The presence, in the primary structure, of four pairs of identical residues, i.e., Phe, Leu, Ile, and Pro, and the similarity of the spectral patterns of the side chains of Leu and Ile made it necessary to perform a redundant number of 2D experiments. The characteristic coupling patterns of the aliphatic protons of Pro, Val, and Phe were readily identified by means of HOHAHA[27] and DQF-COSY[28] spectra. Figure 6 shows a combination of the 500-MHz DQF-COSY and 400-MHz HOHAHA spectra of CLA at 214 K. The more complex patterns of Leu and Ile side chains, together with the identification of the two aromatic subspectra, however, were only possible with the further aid of COSY-relayed[29] and double quantum (DQ)[30] spectra.

The identification of one of the NH resonances (Leu^5) proved particularly arduous. The resonance at ca. 7.26 ppm is in fact a superposition of a triplet corresponding to the 3,5 aromatic protons of one of the Phe residues and of an NH peak, as indicated by integration. However, owing to the very low value of $J_{NHC\alpha H}$ for Leu^5, neither the HOHAHA, the DQF COSY, or the DQ spectra showed any correlation with peaks of the αCH region. Only the NOESY[31] spectrum did show cross peaks corresponding to an αCH at 3.72 ppm.

Sequential assignments, based on NOESY experiments, were also somewhat difficult since the usual COSY–NOESY network was fully visible only in the case of the Phe^4-Leu^5 pair. It was possible however to rely on several other interchain NOEs.

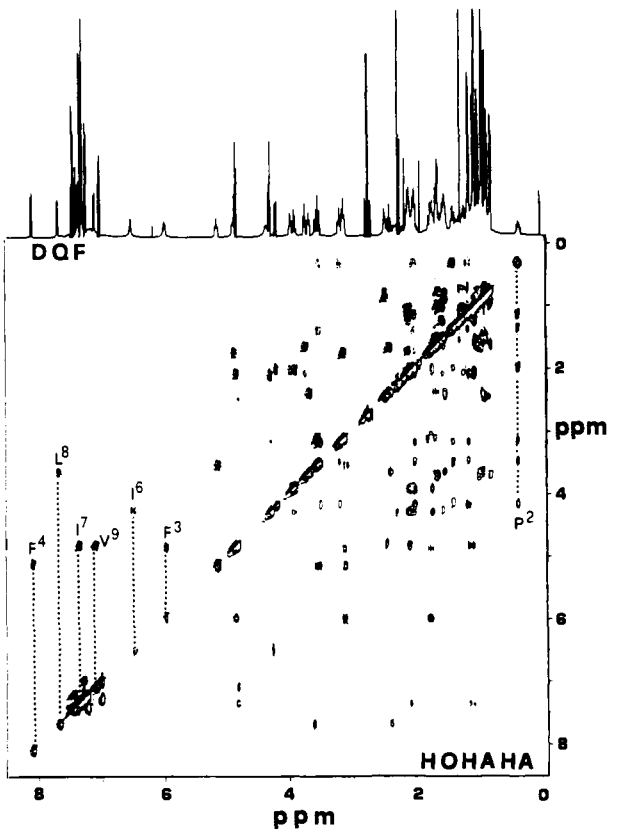

Figure 6. Combined pure absorption double quantum filtered COSY (upper triangle)/homonuclear hartmann–hahn (lower triangle) spectra of 6 mM CLA in $CDCl_3$ at 214 K. Standard single-letter code is used to identify amino acid residues.

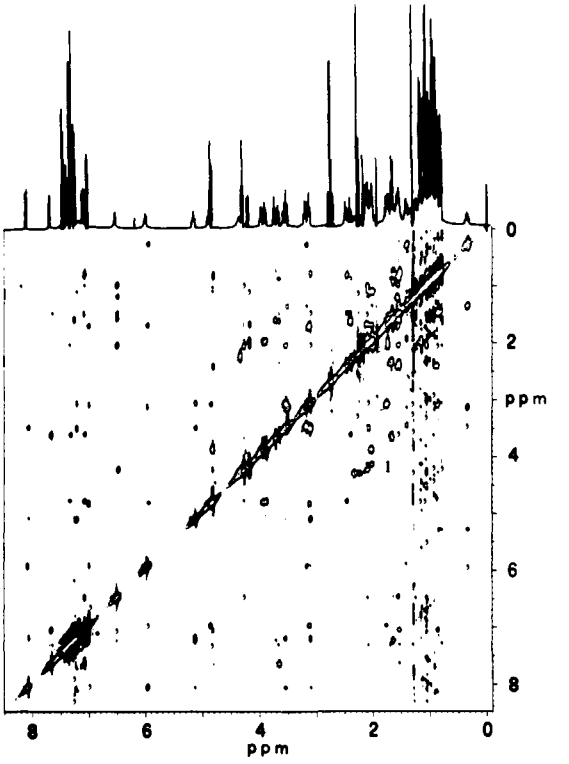

Figure 7. Pure absorption NOESY spectrum of 6 mM CLA in $CDCl_3$ at 214 K performed with a 350-ms mixing time.

Figure 7 shows a 500-MHz NOESY spectrum of CLA at 214 K, performed with a mixing time of 350 ms. The sequence can be followed toward either the C-terminal or the N-terminal direction, starting from the singular Val^9 residue. Strong $d_{\alpha\delta}$ cross

(27) (a) Braunschweiler, L.; Ernst, R. R. *J. Magn. Reson.* **1983**, *53*, 521–528. (b) Davis, D. G.; Bax, A. *J. Am. Chem. Soc.* **1985**, *107*, 2820–2827.
(28) Rance, M.; Sørensen, O. W.; Bodenhausen, G.; Wagner, G.; Ernst, R. R.; Wuthrich, K. *Biochem. Biophys. Res. Commun.* **1983**, *117*, 479–485.
(29) Eich, G.; Bodenhausen, G.; Ernst, R. R. *J. Am. Chem. Soc.* **1982**, *104*, 3732–3740.
(30) Wokaun, A.; Ernst, R. R. *Chem. Phys. Lett.* **1977**, *52*, 407–412.
(31) Macura, S.; Ernst, R. R. *Mol. Phys.* **1979**, *41*, 91–101.

Table V. Chemical Shifts of CLA at 214 K

Pro[1]		Ile[6]	
α	4.27	N	6.50
β	2.09	α	4.28
β′	1.72	β	2.12
γ	2.09	γ	1.51
γ′	2.01	γ′	1.23
δ	3.94	γMet	1.07
δ′	3.88	δMet	1.04
Pro[2]		Ile[7]	
α	4.18	N	7.34
β	2.00	α	4.83
β′	1.15	β	2.09
γ	1.40	γ	1.57
γ′	0.33	γ′	1.23
δ	3.50	γMet	1.15
δ′	3.18	δMet	1.06
Phe[3]		Leu[8]	
N	5.96	N	7.66
α	4.86	α	3.66
β	3.13	β	2.39
$Ar_{2,6}$	6.99	β′	1.65
$Ar_{3,5}$	7.26	γ	1.54
Ar_4	7.37	δ, δ′	0.92
Phe[4]		Val[9]	
N	8.07	N	7.08
α	5.13	α	4.81
β	3.55	β	2.46
β′	3.11	γ	0.88
$Ar_{2,6}$	7.21	γ′	0.85
$Ar_{3,5}$, Ar_4	7.43		
Leu[5]			
N	7.26		
α	3.72		
ββ′γ	1.65		
δ	0.99		
δ′	0.79		

peaks between the α proton of Val[9] and both δ protons of a Pro residue identify Pro[1] in a straightforward way. Proceeding in the C-terminal direction through the Pro[1]-Pro[2] $d_{\alpha\alpha}$ cross peak, it is possible to assign the Phe[3] resonances from $d_{\delta'N}$ and $d_{\gamma'N}$ cross peaks, connecting the high-field γ′ and δ′ protons of Pro[2] to the Phe[3] NH. A d_{NN} cross peak links Phe[3] and Phe[4], and the already-mentioned $d_{\alpha N}$ cross peak leads to Leu[5]. Only a weak d_{NN} cross peak is present between Leu[5] and Ile[6], but no Ile[6]–Ile[7] cross peaks could be identified. However, starting again from Val[9] in the N-terminal direction, a d_{NN} cross peak links Val[9] and Leu[8], and finally a combination of $d_{N\alpha}$ and d_{NN} peaks supports the Ile[7] assignment.

Intraresidue cross peaks allowed a complete assignment of the aromatic resonances of the two Phe residues. The results of the assignment work are summarized in Table V.

Figure 8 shows the 500-MHz 1D ^1H spectrum of 6 mM CLA in chloroform at 214 K, with the explicit indication of all subspectra.

(2) Solution Conformation. Chemical shift values, their temperature dependences, NOEs, and a quantitative evaluation of vicinal coupling constants allow a self-consistent conformational analysis of the backbone conformation of CLA in solution. A partial elucidation of the main conformational features of the side chains was also possible. The spectrum of Figure 8 shows only one set of sharp signals. This observation, together with the temperature behavior, points to a complete conformational homogeneity;[32] i.e., it is possible to exclude both the presence of slowly interconverting cis–trans isomers (around the Xxx-Pro bonds) and fast interconversion among two or more isomers. Chemical shift values for corresponding protons of like amino acids show very large differences, e.g., the NH's of Phe[3] and Phe[4] differ by ca. 2 ppm, those of Ile[6] and Ile[7] by 0.8 ppm, and those of Leu[5] and Leu[8] by 0.4 ppm, respectively. Markedly distinct chemical shifts are exhibited by all diastereotopic proton pairs; the Δδ between the β protons of Phe[3] is 1.4 ppm, while that for Phe[4] is 0.4 ppm. The values for the aliphatic protons of the Pro residues range from a minimum of 0.3 ppm (δ, δ′ protons) to a maximum of 1.1 ppm (γ, γ′ protons) for Pro[2], whereas a maximum value of 0.37 ppm (β, β′) was observed for the pairs of Pro[1]. Moreover, the γ′ proton of Pro[2] experiences an unusually large high-field shift that moves this resonance to 0.33 ppm from TMS. Smaller but still clear indications of the absence of degeneracy are shown by the side-chain protons of all remaining residues (Table V).

The NH–C_αH coupling constants of all NH-bearing residues (with the only exception of Leu[5]) could be measured directly from the one-dimensional spectrum, although they were also double checked in the DQF-COSY.

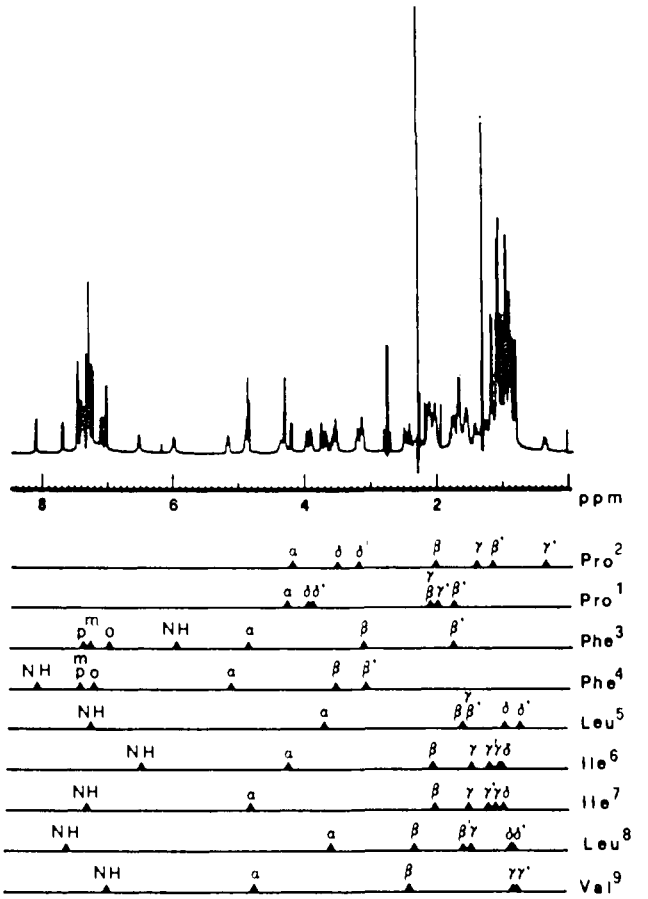

Figure 8. 500-MHz ^1H NMR spectrum of 6 mM CLA in $CDCl_3$ at 214 K, together with subspectra of all amino acid residues. Greek letters identify different types of protons of each residue; o, m, and p symbols stand for the aromatic (2,6), (3,5), and 6 protons of the Phe residues.

Table VI. Vicinal Coupling Constants of CLA in Chloroform at 214 K with the Corresponding φ Angles[33]

	$^3J_{NHC\alpha H}$, Hz	φ, deg
Phe[3]	8.82	50 ÷ 70, −90, −150
Phe[4]	10.01	−100 ÷ −150
Leu[5]	(<2)[a]	(−60 ÷ 0, 120 ÷ 170)[a]
Ile[6]	7.96	35 ÷ 85, −85, −160
Ile[7]	11.02	−110 ÷ −140
Leu[8]	7.81	35 ÷ 85, −85, −160
Val[9]	11.23	−110 ÷ −130

[a] See text.

Table VII. Temperature Dependence of the NH Chemical Shifts ($-\Delta\delta/\Delta T$, ppb/K) of CLA in Chloroform, in the Range 204–264 K

Phe[3]	Phe[4]	Leu[5]	Ile[6]	Ile[7]	Leu[8]	Val[9]
a	0.8	*b*	2.8	1.6	2.0	0.9

[a] Nonlinear. [b] Not observable.

(32) Kessler, H. *Angew. Chem., Int. Ed. Engl.* **1982**, *21*, 512–523.

Table VIII. Theoretical φ Angles in Hydrogen-Bonded β- and Y-Turns[35]

turn	βI	βI′	βII	βII′	γ	γ'
position	$i+1, i+2$	$i+1, i+2$	$i+1, i+2$	$i+1, i+2$	$i+1$	$i+1$
φ, deg	−60, −90	60, 90	−60, 80	60, −80	70 to 85	−70 to −85

Table VI summarizes all measured $J_{NHC_\alpha H}$ values, corrected for electronegativity, together with the corresponding allowed φ angles.[33] The outstanding values of Phe[4], Ile[7], and Val[9] indicate a trans arrangement for the NH–C_αH moieties of Ile[7] and Val[9] and a quasi-trans arrangement for that of Phe[4].

The stereochemistry of the two Xxx–Pro peptide bonds was determined from NOEs. The strong NOE between the two α protons of Pro[1] and Pro[2] and those between Pro[2] CαH and the β and β' protons of Pro[1] are characteristic of a cis Pro[1]–Pro[2] peptide bond; the strong cross peaks connecting Val[9] CαH to the δ,δ' protons of Pro[1], on the other hand, indicate a trans arrangement of the Val[9]–Pro[1] bond.

Information on the NH's involved in hydrogen bonds can be drawn from their temperature coefficients. Stevens et al.,[26] on the basis of a study of rigid models, have shown in fact that, in chloroform, amide protons freely exposed to the solvent have chemical shift temperature coefficient of the order of −2.4 ppb/K; NH's, which remain hydrogen bonded in the whole temperature range examined, have absolute values smaller than 2.4 ppb/K, and NH's that undergo a transition from bound to unbound state in the same temperature range have values larger than 2.4 ppb/K.

Table VII shows the coefficients measured in the chloroform solution of CLA. It is clear that the NH's of Phe[4], Ile[7], Leu[8], and Val[9] can all be regarded as hydrogen bonded in the whole temperature range examined, whereas that of Ile[6] is exposed to the solvent. Nothing can be said for Phe[3] since the nonlinear dependence on temperature shown by its NH indicates that, besides the hydrogen-bond breaking, some other mechanism, e.g., a conformational transition, is influencing the chemical shift. A conformational transition leading to a progressive tightening (when the temperature is lowered) of the portion of CLA containing Phe[3] and Pro[2] is in fact indicated also by the parallel increase of the unusual high-field shift of the γ' proton of Pro[2]. At 214 K this proton is in spatial proximity to Phe[3] NH, as indicated by a cross peak in the NOESY spectrum. The high-field shift of Phe[3] NH, as well as those of β' and γ' protons of Pro[2], can be easily accounted for by the effect of the ring current of the aromatic ring of Phe[3]. This spatial arrangement of the side chains of Pro[2] and Phe[3] is substantiated by NOEs involving Phe[3] NH. In fact, this proton exhibits NOEs with both the 2,6 aromatic protons of Phe[3] and the two γ' and δ' protons of Pro[2]; i.e., it is in a sandwich-type conformation, facing both the Phe[3] aromatic ring and the cyclic Pro[2] side chain. It is fair to assume that this side-chain to side-chain interaction can only be stabilized at the lowest attainable temperature.

The temperature coefficient of Leu[5] NH cannot be measured accurately, since its resonance is always hidden by the triplet of the 3,5 aromatic protons of Phe[3]; nonetheless, from the very fact that the two resonances are always superimposed, it is possible to estimate that the coefficient has to be consistently lower than 2.4.

Should we then consider also Leu[5] NH as intramolecularly hydrogen bonded; all the hydrogen-bonded NH's we find in solution, i.e., Phe[4], Leu[5], Ile[7], Leu[8] and Val[9], coincide with those found in the solid state. This information alone would not be sufficient to tell that the backbone structures in solution and in the solid state are the same, but it is possible to combine it with the information from φ values and from characteristic NOE patterns.[34] All observed NOEs are consistent with the intramolecular proton–proton distances that can be calculated from the solid-state structure. Their analysis in structural terms, however, was done in a completely independent fashion with respect to the solid-state structure, in order to detect possible differences between solution and solid-state conformations.

Let us consider one of the β-turns found in the solid state, i.e., the one involving Phe[4], Leu[5], Ile[6], and Ile[7]. The temperature coefficient of Ile[7] is consistent with the fact that it should be bound to the CO group of Phe[4], but obviously, we cannot tell from these data alone whether this CO is actually bound to the Ile[7] NH. The geometry of the β-turns requires[35] φ angles, for the $i+1$ and $i+2$ positions of the turn, such as shown by Table VIII. The φ value for the $i+2$ position is diagnostic for distinguishing between a type I and a type II turn. The coupling constant for Leu[5] (ca. 2 Hz), although only roughly estimated for lack of resolution, is consistent with a β-turn, since it corresponds to φ ranges of −60° to 0° and 120° to 170°, with respect to a theoretical value of −60° for the $i+1$ position. The experimental φ values for Ile[6] (see Table VI), in the $i+2$ position, would not, per se, allow a distinction between βI and βII turns, being compatible with both theoretical values. Conclusive indication in favor of a type I turn is furnished by the NOE between Phe[4] αCH and Ile[6] NH, which indicates a spatial proximity allowed by the type I turn only.

Similarly, the φ values indicated by the $^3J_{NHC_\alpha H}$ constant of Ile[7], together with the NH–NH cross peak between Ile[7] and Leu[8], are a good indication of the presence of a type I β-turn involving Leu[5], Ile[6], Ile[7], and Leu[8], with a hydrogen bond between Leu[8] NH and the carbonyl of Leu[5]. This conformation is backed by the absence of an NOE between Ile[7] NH and Ile[6] αCH and by the low-field shift of Ile[7] αCH (with respect to the corresponding proton of Ile[6]), since this shift can well be due to the alignment of Ile[7] CH with Ile[6] CO, allowed by the geometry of the turn.

As for the γ'-turn found in the solid state, there are also good indications from our solution data, in spite of the fact that the hydrogen bond involving Leu[5] NH can only be surmised from the persistent coincidence of its NH chemical shift with that of an aromatic resonance (with a very low temperature coefficient). In fact, both the NOE between Phe[4] αCH and Leu[5] NH and the φ ranges for Phe[4], corresponding to the theoretical φ values expected for a γ'-turn, are in favor of the existence of such a turn. The presence of a NOE between Pro[1] αCH and Phe[4] NH, indicative of an inward orientation of this NH, also points in favor of the γ'-turn.

This NOE is also diagnostically valuable for the larger ring that defines the global backbone conformation in the solid state: the C_{13} ring or α-turn, involving Val[9], Pro[1], Pro[2], Phe[3], and Phe[4]. The presence of this ring is strongly supported by the very low temperature coefficient of Val[9] NH (−0.8 ppb/K) and by the NOE cross peak between a Phe[4] β proton and Val[9] methyl protons, since the spatial proximity of these side-chain protons speaks in favor of the involvement of Phe[4] CO as the hydrogen-bond partner of Val[9] NH. Further support comes from the trans arrangement of the NH–CH moiety of Val[9] (from its φ ranges) and from the NOE between Val[9] and Leu[8] NH's. The geometrical constraints imposed by the ring would lead to an alignment of Val[9] αCH and Leu[8] CO, an arrangement similar to that described for the Ile[7]-Leu[8] pair, that leads in fact to similar chemical shift values for Val[9] and Ile[7] αCH's.

The presence of NOEs spatially interconnecting side-chain protons of different residues (inter alia Val[9] β and Leu[8] γ, Phe[4] β and Val[9] γ), is indicative of the presence of a definite conformation also for most of the CLA side chains.

Conclusions

CLA assumes in the solid state a conformation stabilized by five transannular H-bonds of the N–H···O=C type with formation of one γ-turn (C_7), two β-turns (C_{10}, one of type I and one of type III), one α-turn (C_{13}), and one C_{17} ring structure. This structure

(33) Bystrov, F. *Prog. NMR Spectrosc.* **1976**, *10*, 41–82.
(34) Wagner, G.; Newhaus, D.; Worgotter, E.; Vasak, M.; Kagi, J. H. R.; Wuthrich, K. *J. Mol. Biol.* **1986**, *187*, 131–135.
(35) Rose, G. D.; Gierash, L. M.; Smith, J. A. *Adv. Protein Chem.* **1985**, *37*, 1–109.

has also been observed in another crystalline modification[36] obtained from different solvent solutions, which demonstrates that it does represent one of the minimum energy conformations available to this cyclic system.

The results of the conformational analysis in solution by NMR spectroscopy indicate that, provided one choses the right environment, solid-state and solution conformations are essentially identical, in spite of the great tendency of this cyclic molecule to exist in several quasi-isoenergetic conformations. This tendency is favored by the intrinsic flexibility, linked to the cis-trans isomerism of the two Xxx-Pro bonds, and by polar solvents that can divert one or more NH's from the formation of intramolecular hydrogen bonds.

(36) Neela, B. S.; Maujula, M. V.; Ramakumar, S.; Balasubramanian, D.; Viswamitra, M. A. *Biopolymers*, in press.

Registry No. CLA, 33302-55-5; CLA·2Me$_2$CHOH·H$_2$O, 122382-81-4.

Terminal Aminophosphinidene Complexes. A New Approach

François Mercier, Bernard Deschamps, and François Mathey*

Contribution from the Laboratoire de Chimie du Phosphore et des Mêtaux de Transition, DCPH, Ecole Polytechnique, 91128 Palaiseau Cedex, France. *Received March 15, 1989*

Abstract: The thermal decomposition of [1-(diethylamino)-2,3-diphenylphosphirene]pentacarbonyltungsten at ca. 130 °C provides an access to transient [(diethylamino)phosphinidene]pentacarbonyltungsten [Et_2N—P=$W(CO)_5$]. This transient phosphinidene complex is trapped by 2,3-dimethylbutadiene, ethanol, and diethylamine to give the expected adducts. Similarly, [1-(diethylamino)phosphirane]pentacarbonyltungsten yields the same phosphinidene complex above 50 °C. In that case, the trapping experiments have been carried out with phenylacetylene, tolan, 2,3-dimethylbutadiene, and 1-hexene. Neither 1-alkyl- nor 1-arylphosphirene and -phosphirane P–$W(CO)_5$ complexes are efficient precursors of terminal phosphinidene complexes. The reason why 1-amino substituents so much improve the situation is thought to be the stabilization of the first singlet state of terminal aminophosphinidene complexes [R_2N—P=$W(CO)_5$] by comparison with their alkyl or aryl counterparts. The reaction of [1-(diethylamino)phosphirane]pentacarbonyltungsten with HCl yields the corresponding 1-chlorophosphirane complex. This complex in turn can be used as a precursor for (chlorophosphinidene)pentacarbonyltungsten [ClP=$W(CO)_5$] above 100 °C.

As carbene complexes $R_2C{=}ML_n$ (Fischer and Schrock types), terminal phosphinidene complexes $RP{=}ML_n$ can be divided into two subclasses according to their electrophilicity or their nucleophilicity. The electrophilic type can be viewed as a metallophosphenium cation $RP^+{-}M^-L_n$ and its chemistry resembles that of electrophilic carbenes.[1] The nucleophilic type is polarized in the opposite direction $R^{\delta-}P{=}M^{\delta+}L_n$ and is synthetically equivalent to RP^{2-}. Recently, Lappert[2] has described stable examples of the nucleophilic type. On the contrary, until now, no stable example of the electrophilic type has been reported in the literature. A priori, stabilization could be achieved with bulky substituents and reduced electrophilicity. Meeting such criteria, bulky aminophosphinidene complexes appear as a promising solution. Two results from the literature strengthen this opinion. Cowley[3] has shown that it is possible to stabilize an electrophilic phosphinidene $Fe(CO)_4$ complex by self-complexation with an internal tertiary amino group. Besides, Gladysz and Bertrand[4] have detected a bulky cationic [(diisopropylamino)phosphinidene]iron complex at low temperature by ^{31}P NMR. This species collapses via the insertion of phosphorus into one of the C–H bonds of the diisopropylamino group when raising the temperature. A more thorough study of terminal aminophosphinidene complexes appears all the more interesting since, as synthetic tools, they can be viewed as equivalent to masked halogenophosphinidene or unsubstituted phosphinidene complexes via a series of classical transformations carried out on the end products resulting from their chemistry (eq 1).

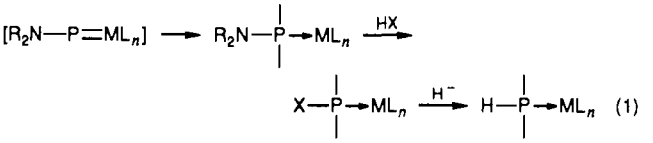

(1)

Results and Discussion

The now classical route to terminal phosphinidene complexes using 7-phosphanorbornadiene complexes as precursors[1] is of no use in the case of aminophosphinidene complexes because side reactions take place between the P–N bond and dimethyl acetylenedicarboxylate (eq 2). We thus turned our attention toward

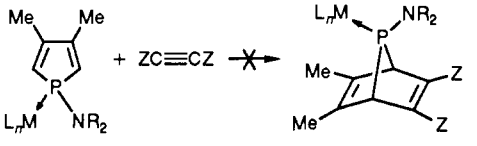

(2)

Z = CO_2Me

(1) This chemistry has been described in a recent review: Mathey, F. *Angew. Chem., Int. Ed. Engl.* **1987**, *26*, 275. Another recent review deals more with theoretical aspects: Cowley, A. H.; Barron, A. R. *Acc. Chem. Res.* **1988**, *21*, 81. Since the appearance of these two reviews, several new developments have been reported concerning the insertion into 3-membered rings, the reaction with carbene and carbyne complexes, the insertion into clusters, and the exchange of substituents; see: Marinetti, A.; Mathey, F. *Organometallics* **1987**, *6*, 2189. Tran Huy, N. H.; Ricard, L.; Mathey, F. *Organometallics* **1988**, *7*, 1791. Tran Huy, N. H.; Fischer, J.; Mathey, F. *Organometallics* **1988**, *7*, 240. de Vaumas, R.; Marinetti, A.; Mathey, F.; Ricard, L. *J. Chem. Soc., Chem. Commun.* **1988**, 1325. Holand, S.; Mathey, F. *Organometallics* **1988**, *7*, 1796. On the other hand, a kinetic study of the reactions of [PhP=$W(CO)_5$] with a series of para-substituted styrenes has shown that it behaves as a mild electrophile somewhat similar to a vinylidenecarbene; see: Lammertsma, K.; Chand, P.; Yang, S.-W.; Hung, J.-Te *Organometallics* **1988**, *7*, 1875.

(2) Hitchcock, P. B.; Lappert, M. F.; Leung, W.-P. *J. Chem. Soc., Chem. Commun.* **1987**, 1282.

(3) Cowley, A. H.; Geerts, R. L.; Nunn, C. M. *J. Am. Chem. Soc.* **1987**, *109*, 6523.

(4) Nakazawa, H.; Buhro, W. E.; Bertrand, G.; Gladysz, J. A. *Inorg. Chem.* **1984**, *23*, 3431.

0002-7863/89/1511-9098$01.50/0